TAMPERE UNIVERSITY OF TECHNOLOGY

Application of Hill-Clohessy-Wiltshire Equation in GNSS Orbit Prediction

Application of the Hill-Clohessy-Wiltshire equation in GNSS orbit prediction

Xiaolong Zhang and Robert Piché
Tampere University of Technology, Finland
Email: {xiaolong.zhang, robert.piche}@tut.fi

Abstract— We present an initial state correction algorithm for GNSS orbit prediction that uses the solution of the Hill-Clohessy-Wiltshire (HCW) equation to build the Jacobian matrix. This algorithm improves the accuracy of GNSS orbit prediction through adding one or more observations. In the tests of 14 days orbit prediction, by adding one broadcast ephemerides (BE) as an observation collected before the initial BE with a proper interval, we get orbit-only User Range Error within 70 meters, and orbit errors in the radial direction is less than 15 meters. In tangential direction, the error is within 400 meters.

I. Introduction

Even in an ideal case, a stand-alone GNSS receiver needs at least 30 seconds to receive the orbit data needed for positioning. If the receiver is moving or the sky view is obstructed by trees or buildings, then the time to first fix (TTFF) can even be up to several minutes, and positioning is not possible at all in deep inside buildings.

Orbit prediction ("nowcasting") for GNSS satellites from broadcast ephemerides (BE) can be used to reduce TTFF by generating orbit data on the device. This technology is especially useful as an alternative to positioning assistance data obtained through a network connection [1], [2].

In this method, the device continually stores some broadcast ephemerides. Then, when the device is turned on again some hours or days after the last use, and new ephemeris data are needed, satellites' orbits are propagated forward to the current epoch by solving the differential equation of motion. On current smart mobile devices, several days' orbit propagations for a whole GNSS constellation can be computed within a few seconds. Numerical orbit propagation can provide more accurate results than analytical or semi-analytical orbit prediction, since it can apply more accurate force models.

In order to accurately compute a GNSS satellite orbit, it is necessary to correct the BE's initial orbital state [3], [4]. Seppänen et al.[3] used an iterative nonlinear least squares algorithm to fit the force model's orbit to points on the BE's orbit. This process normally requires building a Jacobian matrix, this matrix reflects how small disturbances in an initial state will affect the state in the future epoch, but building this matrix numerically is computationally heavy. Since the orbits of GPS and Glonass satellites are nearly circular, their eccentricity being smaller than 0.02 and 0.003 respectively, they satisfy the assumption of the Hill-Clohessy-Wiltshire (HCW) equation. We can use this equation to describe the deviation trend of GNSS satellite' orbit caused by the initial state's error. Using the analytical formula for the solution of the HCW equation is more efficient for correction of an orbit initial state than using numerically computed Jacobian matrices. In this paper we describe in detail the algorithm of how to correct the initial state with two or more points of Glonass BE. Furthermore, results of an extensive series of tests for Glonass orbit prediction are also presented.

II. Force Model

The motion of a satellite under the influence of a force F is described by the differential equation

$$\ddot{\vec{r}} = F(t, r, v)/m \qquad (1)$$

where r and v are the position and the velocity of the satellite in a non-rotating geocentric coordinate system, m is the satellite's mass, and t is time. The force model considered in this work includes four major forces: the Earth, Sun and Moon gravity, and solar radiation pressure (SRP). Then the equation of motion (1) can be written as

$$\vec{a} = \vec{a}_{\text{Earth}} + \vec{a}_{\text{Moon}} + \vec{a}_{\text{Sun}} + \vec{a}_{\text{srp}} \qquad (2)$$

We use EMG2008 as our Earth gravity model, taking terms up to degree and order 8; the geo-potential coefficients are published by National Geospatial-Intelligence Agency [5]. Moon and Sun are modeled as point masses.

For SRP, we use a two-parameter empirical model whose parameters are fitted offline using long term precise orbit data; details are in [6].

III. Reference Frame

A. Coordinate transform between ITRF and ICRF

The broadcast ephemeris's state of orbit is given in ECEF (Earth-Centered, Earth-Fixed) frame, e.g. GPS's WGS84 and Glonass's PZ-90.02. Both of these reference systems are consistent with the International Terrestrial Reference Frame (ITRF) that is maintained by International Earth Rotation and Reference Systems Service [7]. The newest version of ITRF has only a centimeter level of offset with WGS84. PZ-90.02 is consistent with ITRF in a decimeter level, and it has only an offset in position [8] given by

$$\begin{pmatrix} x \\ y \\ z \end{pmatrix}_{\text{ITRF}} = \begin{pmatrix} x \\ y \\ z \end{pmatrix}_{\text{PZ-90.02}} + \begin{pmatrix} -0.36 \text{ m} \\ 0.08 \text{ m} \\ 0.18 \text{ m} \end{pmatrix} \qquad (3)$$

After PZ-90.02 is corrected for the offset, we regard all the Terrestrial Reference Frames as same, denoted as TRF.

Orbit propagation computations are carried out in International Celestial Reference Frame (ICRF). The transformation between TRF and ICRF is [9]

$$\vec{r}_{\text{ICRF}}(t) = P(t)N(t)R(t)W(t)\vec{r}_{\text{TRF}} \tag{4}$$

where P and N are the precession and nutation matrix at time t, R is the Earth rotation matrix, and W is polar motion matrix. The transformation is based on IAU-1976 Theory of Precession and IAU-1980 Theory of Nutation. During the orbit propagation, we keep P, N and W as constant because, during one week, these three matrices are almost unchanged; the difference of disturbance forces after this simplification is several orders of magnitude smaller than the smallest term in our force model. This arrangement will not significantly degrade the precision of the orbit integration in inertial frame, it produces only few meters error when transformed back to TRF. In this paper, orbit analysis is carried out in RTN (Radial, Tangential and Normal) reference frame, not in TRF, so the analysis results will not be affected.

We choose an intermediate inertial frame, which is not ICRF at epoch J2000, but is TRF at the start epoch t_0 [3].
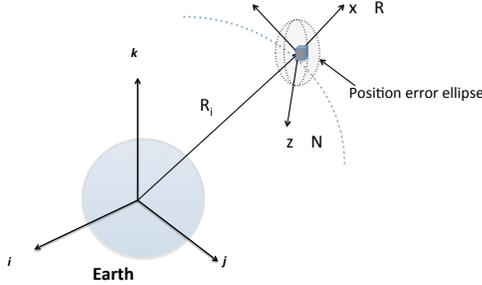
B. Hill reference frame

Fig. 1. Hill Frame

The origin of the Hill frame is in the mass center of satellite. x direction is aligned with the direction of Earth to satellite; the y direction is in the orbit plane and perpendicular to x, and positive in the direction of satellite motion; z completes the right-handed triad. We also call the axis of Hill frame as Radial (R), Tangential (T), and Normal (N) direction, as indicated in the figure above.

IV. HILL-CLOHESSY-WILTSHIRE EQUATION

The HCW equation describes the motion of a body relative to a reference orbit that is circular or nearly circular. Although HCW equation is linearized and without disturbance force, it can provide approximations of the Jacobian for our purposes. The HCW equations used in this work are [10]

$$\begin{aligned} \ddot{x} &= 3n^2x + 2n\dot{y} \\ \ddot{y} &= -2n\dot{x} \\ \ddot{z} &= -n^2z \end{aligned} \tag{5}$$

where x, y, z are the coordinates in Hill's frame described in Fig. 1, and n is the mean motion of reference orbit; $n \approx 1.550 \times 10^{-4}$ radian/s for Glonass satellites. The closed form solution of (5) is

$$X(t_{i+1}) = \Phi X(t_i) \tag{6}$$

where $X(t_i) = [x\ y\ z\ \dot{x}\ \dot{y}\ \dot{z}]^T$ is the state at epoch t_i in Hill's frame, and

$$\Phi = \begin{bmatrix} \phi_{11} & \phi_{12} \\ \phi_{21} & \phi_{22} \end{bmatrix} \tag{7}$$

with

$$\phi_{11} = \begin{bmatrix} 4 - 3\cos n\delta & 0 & 0 \\ 6(\sin n\delta - n\delta) & 1 & 0 \\ 0 & 0 & \cos n\delta \end{bmatrix} \tag{8}$$

$$\phi_{12} = \begin{bmatrix} (\sin n\delta)/n & 2(1 - \cos n\delta)/n & 0 \\ 2(\cos n\delta - 1)/n & (4\sin n\delta - 3n\delta)/n & 0 \\ 0 & 0 & (\sin n\delta)/n \end{bmatrix} \tag{9}$$

$$\phi_{21} = \begin{bmatrix} 3n\sin n\delta & 0 & 0 \\ 6n(\cos n\delta - 1) & 0 & 0 \\ 0 & 0 & -n\sin n\delta \end{bmatrix} \tag{10}$$

and

$$\phi_{22} = \begin{bmatrix} \cos n\delta & 2\sin n\delta & 0 \\ -2\sin n\delta & 4\cos n\delta - 3 & 0 \\ 0 & 0 & \cos n\delta \end{bmatrix} \tag{11}$$

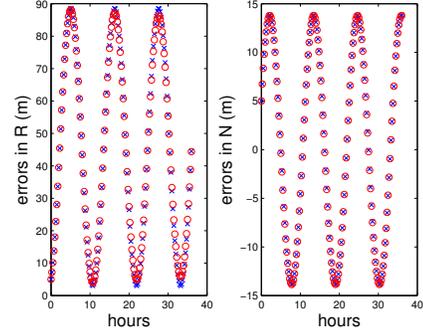and $\delta = t_{i+1} - t_i$ is the time step size..

Fig. 2. Position errors in Radial and Normal direction

Figures 2 and 3 show how the solution of HCW can capture the relative motion for a GNSS satellite. We choose an initial state of Glonass satellite PRN 8 from its BE at 00:15:00 11th Aug 2013, and add to it a perturbation $[5\text{ m}\ 5\text{ m}\ 5\text{ m}\ 0.002\text{ m/s}\ 0.002\text{ m/s}\ 0.002\text{ m/s}]^T$ in Hill's frame, to generate another initial state. We then propagate the states forward 36 hours using numerical integration of the full force model and plot the differences of the two trajectories in Hill's frame as blue crosses. The origin of this Hill's frame is the mass center of the first satellite. The red circles indicate the results that directly use (6) to predict the relative motion caused by the perturbation. Motion in radial and normal direction is stable, as seen in Fig. 2. Both of them are only sinusoidal oscillation. From the formulas (8–9) for ϕ_{11} and ϕ_{12}, we see that the motion in the tangential
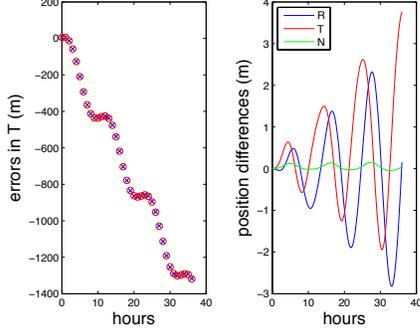
Fig. 3. Left part shows the position error in Tangential direction, and the right part is the differences between numerically and analytically computed error in Tangential direction.

direction is unstable, it drifts with a secular term. The left of Fig. 3 also shows this unstable motion. The right part of this figure indicates the differences between the perturbed trajectory and the trajectory that is analytically computed with Hill's equation. These differences are small relative to the magnitude of their drift and oscillation.

A. Initial state correction

For a Glonass satellite, if we directly propagate its orbit forward one week with its BE, then because of inaccuracies in position and especially in velocity, the position error will increase up to tens of meters in the radial and normal direction, and in the tangential direction, the position error can easily grow to more than 1000 meters. Glonass's BE is only valid within 30 minutes [11]. This is too short to correct the initial state because the orbit prediction error caused by initial uncertainties cannot be distinguished from the noise of the BE. We therefore use more than one BE to correct the initial state. The procedure is described in the following.

The force model is used to propagate the initial point backward, and the trajectory is compared with the BEs at time t_i for $i = 1 \ldots n$. We denote the BE's position as $\vec{r}_{oi}$, and the propagated position as $\vec{r}_{ci}$. We minimize the sum of squares using the cost function

$$J = \sum_{i=1}^{n} \|\vec{r}_{oi} - \vec{r}_{ci}\|^2 \qquad (12)$$

Setting the derivative of J with respect to the initial state $\vec{X}_{t0} = [x \ y \ z \ \dot{x} \ \dot{y} \ \dot{z}]_{t0}^T$ to zero gives the equations

$$\frac{\partial J}{\partial \vec{X}_{t0}} = \sum_{i=1}^{n} \frac{\partial(\vec{r}_{oi} - \vec{r}_{ci})^T}{\partial \vec{X}_{t0}}(\vec{r}_{oi} - \vec{r}_{ci}) = 0 \qquad (13)$$

Here $\frac{\partial(\vec{r}_{oi} - \vec{r}_{ci})^T}{\partial \vec{X}_{t0}}$ is the Jacobian, which describes the relative motion with respect to the initial state in Hill's frame, so it is $[\phi_{11} \quad \phi_{12}]_{t_i - t_0}^T$, denote as A_i^T; ϕ_{11}, ϕ_{12} are given by (8– 9).

Computing $\vec{r}_{ci}$ about a nominal initial state $\vec{X}_n$ using Taylor series, neglecting higher powers of $\Delta\vec{X} = \vec{X}_c - \vec{X}_n$ (second

order and above), and using $\vec{r}_{ni}$ to denote the nominal position at time t_i, we obtain

$$\vec{r}_{ci} = \vec{r}_{ni} + \frac{\partial \vec{r}_{ni}}{\partial \vec{X}_n^T} \Delta\vec{X}$$
$$= \vec{r}_{ni} + A_i \Delta\vec{X} \qquad (14)$$

Substituting (14) into (13), we get

$$\sum_{i=1}^{n} A_i^T(\vec{r}_{oi} - \vec{r}_{ni} - A_i\Delta\vec{X}) = 0 \qquad (15)$$

Let $\hat{r}_i = \vec{r}_{oi} - \vec{r}_{ni}$ denote the position residual and let $\delta\hat{x}$ denote $\Delta\vec{X}$ during the iteration. Then (15) can be written as

$$\sum_{i=1}^{n} (-A_i^T \hat{r}_i + A_i^T A_i \delta\hat{x}) = 0 \qquad (16)$$

The correction to the initial state is

$$\delta\hat{x} = (\sum_{i=1}^{n} A_i^T A_i)^{-1}(\sum_{i=1}^{n} A_i^T \hat{r}_i) \quad n \geq 2 \qquad (17)$$

For our implementation, the predicted position error mainly comes from the error in the T direction. This error is mainly contributed from the initial state's position error in R direction and velocity error in T direction. In tests, we found for Glonass BE that the velocity's error in initial state contribute more than position's error to the prediction errors.

Each matrix of $A_i^T A_i$ in (17) only has a rank of 3, so if we want to get both position and velocity correction, at least 2 observation points must be introduced. If only one more ephemeris is available, we can generate more orbit points using Glonass ICD's [11] simple model within 30 minutes. As mentioned previously, these generated orbit points can only provide little extra information for initial state fitting.

If we only consider correcting the initial state's velocity, assume the position uncertainty is zero. In (17), the partial derivative matrix A_i can be further simplified to $A_i = \phi_{12}$. Then, denoting the velocity correction as $\delta\hat{v}$, the correction to initial velocity is

$$\delta\hat{v} = (\sum_{i=1}^{n} A_i^T A_i)^{-1}(\sum_{i=1}^{n} A_i^T \hat{r}_i) \quad n \geq 1 \qquad (18)$$

where $A_i = \phi_{12}$.

If we only use one BE as observation, then (18) can be written as

$$\delta\hat{v} = (A_i^T A_i)^{-1} A_i^T \hat{r}_i$$
$$= (A_i)^{-1} \hat{r}_i \qquad (19)$$

The initial condition correction iteration is stopped when

$$rms = \sqrt{\frac{1}{n} \sum_{i=1}^{n} \|\delta\hat{r}_i\|^2} < tol \qquad (20)$$

In tests, one or two iterations provides enough prediction accuracy.

V. Tests

A. Test conditions

From 2013-01-01 to 2013-12-31, Glonass satellite's BE as initial points at epoch time 00:15:00 were collected, denoted as IN0. The BEs from 6 and 12.5 hours back are collected as observations, denoted as O1 and O2, respectively. We manually removed aberrant entries from this set of BE triples, as follows. First, we removed the items if any of the IN0, O1 or O2 is unhealthy. Secondly, we removed the ones having invalid epoch time, t_b. For example, in 2013-08-04, the expected BE's epoch time for PRN 23 is 00:15:00, but in the broadcast data file brdc2160.13g, it is 00:15:01.80. Third, if the satellite had a maneuver in the following 14 days, its BE was removed. For example, PRN 19 had a maneuver in the 5th day of GPS week 1755. According to Glonass's Information Analytical Centre [12], a new satellite was inserted into slot 2 on 2013-07-04, and Glonass-M #743 (orbital slot 2) started to maneuver to orbital slot 8 from 2013-01-04. During that maneuver its BEs was marked as unhealthy for more than 2 months in the beginning of 2013. PRN 2 and PRN 8's BEs were therefore removed from tests.

The orbit position reported in the BE is the position of the satellite's antenna center and needs to be translated to the satellite's mass center [3], [13]. We compare our prediction results with IGS's (International GNSS Service) precise orbit product. The product for Glonass's orbit is given in ITRF reference frame with GPS time. But Glonass's BE give orbit in their own PZ-90.02 reference frame with UTC (Coordinated Universal Time) time. The difference between GPS time and UTC time is the leap seconds, currently 16 seconds. After antenna correction, we used (3) to transform Glonass's orbit to ITRF, and propagated Glonass's orbits forward 16 seconds with our full force models.

After the processes mentioned above, we have 6949 BE triples from 22 Glonass satellites over one year. Initial points are propagated backward 12.5 hours or 6 hours, depending which observation points are chosen, and the initial state is corrected using the algorithm described in Section IV. Finally with the converged initial state we predict 2 weeks forward. The errors of the predictions with IGS's precise orbit are described in Hill's frame.

The orbit from Glonass's BE can be propagated 15 minutes before and after the epoch. By Glonass ICD's algorithm propagate satellite orbit to time t, $t = t_b \pm 15$ minutes, two more observed points are created. In the Table of test conditions, "extended obs" means that we use two points at $t_b \pm 15$ minutes also as observations. In the column "BE as obs", O2 means we used the observation from the BE of 12.5 hours back, and O1 is the BE of 6 hours backward.

B. SIS error metrics

Glonass's receiver may have different UREs (User Range Error) at different locations on Earth. Global-average rms URE is given in [14] by

$$\text{rms } URE = \sqrt{(0.98R - C)^2 + (T^2 + N^2)/45} \qquad (21)$$

TABLE I
Test conditions

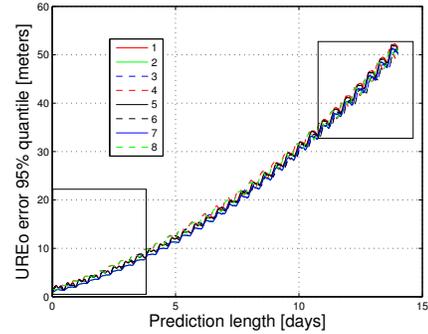| case	correction	BE as obs	extended obs
1	velocity	O2	no
2	velocity	O1,O2	no
3	velocity	O1	no
4	velocity, positon	O1,O2	no
5	velocity	O2	yes
6	velocity	O1	yes
7	velocity	O1,O2	yes
8	velocity, position	O1,O2	yes

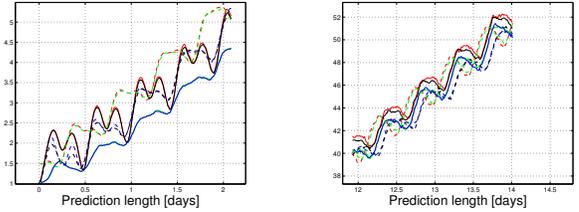Fig. 4.   average rms URE (orbit only)

Fig. 5.   Detail of Figure 4.

where R, T, and N are the error in radial, tangential and normal direction, and C is the clock error. Because we have no precise data for clock error, we only show the orbit-only UREo [14],

$$\text{rms } UREo = \sqrt{(0.98R)^2 + (T^2 + N^2)/45} \qquad (22)$$

C. Results

We used (22) to convert the predicted error in R, T and N to the orbit-only SIS UREo for each predicted point. We grouped these SIS UREo according to the interval between their epoch time and the time of starting orbit prediction. Each group has 6949 UREo values. The 95% quantile of each group as a function of time is plotted in Fig. 4 and Fig. 5. The enlarged part of the beginning and end of Fig. 4 are shown in the left and right of Fig. 5, respectively.

From table I and Fig. 5 we see that all the 8 cases give similar results; the maximum differences are less than 2 meters within 2 weeks predictions. Correction of initial

state's position is unnecessary: comparing case 2 and case 4 ,8 we found that better results are achieved without position correction. In other tests, the introduction of 4 or 5 more BEs as observations inside a 12.5 hour interval also show some results that support this point.

The introduction of more BE as observation will improve accuracy. Comparing cases 2,7 with cases 1,3,5,6, we see that cases 2 and 7 get the best prediction results, especially in the beginning of the predictions. Cases 2 and 7 use two BEs as observations, whereas cases 1 and 5 use only one BE with epoch 12.5 hours back, and cases 3, 6 use one BE with epoch 6 hours back.

The length of the time interval between the initial point and the observations is an important factor for prediction accuracy. In [4], it was found that if this time interval is bigger than 6 hours, the prediction accuracy is more stable. The reason might be that the observation should be introduced far enough away from the initial point to let the prediction error be distinguished from noise in the state correction phase. Further, it was found that if this time interval is close to an integer time of the orbit period, the results are better. This may indicate that our force model may have some error of long period items. For example, the Solar radiation pressure might be inaccurate. The Sun elevation angle, which is the angle between Sun's direction vector and satellite's orbit plane, changes $1°$ per day, and it influences the SRP. Compared with Glonass's orbit period of 11h15m, SRP variation is a long-term. Considering the visibilities of satellites for a receiver local in some area, choosing the observation of around 12 hours back is more feasible.

Extending BEs through Glonass ICD's algorithm is also unnecessary, the lines with and without BEs extended are nearly overlap in Fig. 4 and Fig. 5.
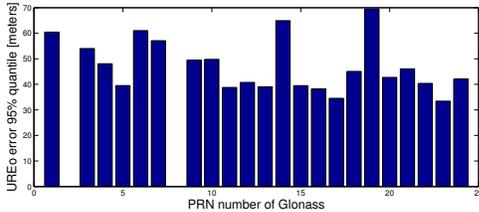

Fig. 6. Maximum value of 95% quantile of UREo for 14 days prediction, with one of 12.5 hours backward BE to correct initial velocity.

Fig. 6 shows the maximum value of 95% quantile of UREo for Glonass' s 22 satellites. As explained in section V.A, PRN 2 and PRN 8 are not included. All the initial velocities are corrected by the BEs of 12.5 hours back. For each satellite's 95% quantile, more than 300 trajectories of 14 days prediction are used. It can be seen that PRN 19 and PRN 14 have bigger UREo than others. Both of them had an orbital maneuver in 2013, and the quality of orbit information from BEs was relatively low after the maneuver, and this lasted some days. The only other maneuver happened to PRN 20 during 2013, but its orbit predictions seem not to be affected by this.

VI. DISCUSSION AND CONCLUSION

A. Discussion

The algorithm for correction of orbit initial state presented in this paper only needs to propagate one trajectory back in every iteration loop; the Jacobian matrix is built analytically, and more than one observation can be included. By contrast, if numerical orbit propagation is used to build the Jacobian, it needs 9 more numerical trajectories for velocity correction. If more observation BEs are introduced, each BEs' Jacobian is built numerically, and the computational load is even heavier. Furthermore, the new algorithm converge quickly, only needing one iteration for velocity correction if one observation is included. If more observations are added, 2 iterations provide enough accuracy.

For the orbit predictions, in this paper we do not consider the eclipse boundary's effects on the integrator. The integrator for the tests in the paper is Gauss-Jackson 8th order with a time step of 900 seconds. When satellites cross the border of the Earth's shadow, we don't restart the integrator or do some modifications to the state, and this might make the prediction results a little worse. GNSS satellite have the noon-turn and midnight-turn during their eclipse season, which are attitude maneuvers at each day's noon and midnight. This also effects the orbit prediction, but in the tests of this paper we do not adjust also. If the prediction trajectories corresponding to eclipses are removed from the test set, the results will be improved a little.

The prediction span of 14 days for GNSS satellites is longer than most of practically implementations, because clock error can be expected to dominate after 4 days [15]. Maybe more than 80% of prediction requirements for GNSS orbits are within 3 days in shortening TTFF.
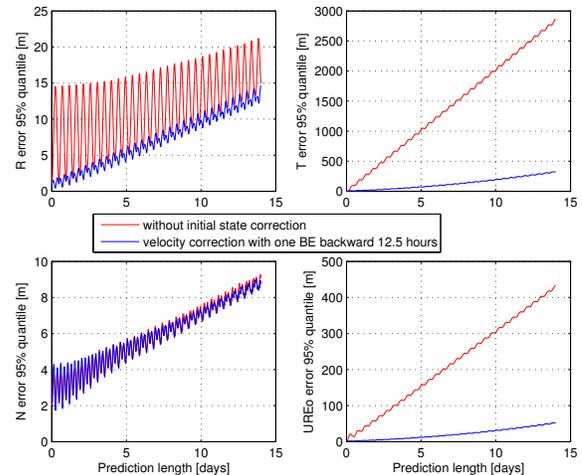

Fig. 7. 95% quantile in R, T, N direction and UREo with and without initial state correction

Fig. 7 shows that through adding one more BE for Glonass orbit prediction, we can decrease the magnitude of the error's

oscillation in R direction, and the error in T direction reduced from thousands of meters to hundreds of meters. But we still notice that the error in R and N direction increase less than 1 meter per day in prediction. This is because our force models are simplified, some disturbances forces are not included, and SRP model may not be accurate enough. According to the solution of HCW, in R and T direction, the orbit should be stable, the uncertainties of initial state only cause oscillations. Further research will try to improve our force models in a trade off between prediction accuracy and computation load.

B. Conclusion

For the initial state correction in GNSS orbit prediction, computing the Jacobian analytically through HCW's motion model is computationally efficient. The initial state correction computation is at least 9 times than numerical algorithm, which is implemented in [3]. In tests, we found that initial position correction is unnecessary. Also, we found that extending Glonass BE through the simple model provided by Glonass ICD does not improve the accuracy of prediction. In the tests of 14 days orbit prediction, by adding one BE as an observation collected before the initial BE with a proper interval, we get UREo within 70 meters, and orbit errors in the radial direction is less than 15 meters. In tangential direction, the error is within 400 meters.

ACKNOWLEDGMENT

REFERENCES

[1] P. G. Mattos, "Hotstart every time-compute the ephemeris on the mobile," in *Proceedings of the 21st International Technical Meeting of the Satellite Division of The Institute of Navigation (ION GNSS 2008)*, 2001, pp. 204–211.

[2] M. Lytvyn, A. Kemetinger, and P. Berglez, "How can an orbit prediction module speed up the TTFF and help to authenticate the position?" in *Satellite Navigation Technologies and European Workshop on GNSS Signals and Signal Processing,(NAVITEC), 2012 6th ESA Workshop on*. IEEE, 2012, pp. 1–6.

[3] M. Seppänen, J. Ala-Luhtala, R. Piché, S. Martikainen, and S. Ali-Löytty, "Autonomous prediction of GPS and GLONASS satellite orbits," *NAVIGATION*, vol. 59, no. 2, pp. 119–134, 2012.

[4] J. Ala-Luhtala, M. Seppänen, S. Ali-Löytty, R. Piché, and H. Nurminen, "Estimation of initial state and model parameters for autonomous GNSS orbit prediction," in *International Global Navigation Satellite Systems Society Symposium 2013 (IGNSS2013)*, July 2013.

[5] (2013) The NGA Earth Gravitational Model 2008 website. [Online]. Available: http://earth-info.nga.mil/GandG/wgs84/gravitymod/egm2008/

[6] J. Ala-Luhtala, M. Seppanen, and R. Piché, "An empirical solar radiation pressure model for autonomous GNSS orbit prediction," in *Position Location and Navigation Symposium (PLANS), 2012 IEEE/ION*. IEEE, 2012, pp. 568–575.

[7] (2014) The IERS product/data website. [Online]. Available: http://www.iers.org/IERS/EN/DataProducts/data.html

[8] S. Revnivykh, "Glonass status and progress," in *Proc. ION GNSS*, 2010, pp. 609–633.

[9] O. Montenbruck and E. Gill, *Satellite orbits*. Springer, 2000.

[10] D. A. Vallado, *Fundamentals of astrodynamics and applications, Fourth Edition*. Microcosm Press, 2013, pp. 393–397.

[11] "Glonass Interface Control Document 5.1," Russian Institute of Space Device Engineering, Tech. Rep., 2008.

[12] (2014) The Glonass's Information Analytical Centre website. [Online]. Available: http://glonass-iac.ru/en/index.php

[13] (2014) The IGS antenna offset website. [Online]. Available: http://igscb.jpl.nasa.gov/igscb/station/general/igs05.atx

[14] L. Heng, G. X. Gao, T. Walter, and P. Enge, "Statistical characterization of glonass broadcast ephemeris errors," in *Proceedings of the 24th international technical meeting of the satellite division of the institute of navigation (ION GNSS 2011), Portland, OR*, 2011, pp. 3109–3117.

[15] S. Martikainen, R. Piché, and S. Ali-Löytty, "Outlier-robust estimation of gps satellite clock offsets," in *2012 International Conference on Localization and GNSS ICL-GNSS, June 25-27, 2012, Starnberg, Germany*, 2012.